

See discussions, stats, and author profiles for this publication at: <https://www.researchgate.net/publication/343624333>

# Isothermal annealing study of the EH1 and EH3 levels in n-type 4H-SiC

Article in *Journal of Physics Condensed Matter* · August 2020

DOI: 10.1088/1361-648X/abaeaf

---

CITATIONS

3

READS

32

2 authors, including:



Giovanni Alfieri

Hitachi ABB Power Grids

114 PUBLICATIONS 1,110 CITATIONS

SEE PROFILE

Some of the authors of this publication are also working on these related projects:



Center for III-Nitride Technology C3NiT - Janzen [View project](#)



Selected-area electrical-doping of wide band-gap semiconductors materials by ion implantation [View project](#)

# Isothermal Annealing Study of the EH1 and EH3 Levels in n-type 4H-SiC

G. Alfieri, A. Mihaila

ABB Power Grids Switzerland Ltd., Segelhofstrasse 1A, 5405 Baden-Dättwil,  
Switzerland

E-mail: [giovanni.alfieri@hitachi-powergrids.com](mailto:giovanni.alfieri@hitachi-powergrids.com)

July 2020

**Abstract.** Particle irradiation is known to give rise to several majority carrier traps in the band gap of n-type 4H-SiC, in the 0.4-1.6 eV energy range below the conduction band edge ( $E_C$ ). Among these traps, the EH1 ( $E_C$ -0.4 eV) and the EH3 ( $E_C$ -0.7 eV) are the least thermally stable ones and not much is known on their microscopic origin. In order to understand the nature of EH1 and EH3, their annealing kinetics was studied by means of deep level transient spectroscopy and the results were interpreted by invoking the diffusion-limited theory. It is found that EH1 and EH3 are two different charge states of the same defect, labeled EH-center, that anneals out with an activation energy of  $\sim 1.1$  eV and whose nature is related to a carbon interstitial. Our study shows that the EH-center is not the same as the S-center defect which was reported by previous studies found in the literature.

## 1. Introduction

Electronic devices for solar cells, on-board satellite electronics and detectors for astronomical imaging must withstand harsh conditions, like high-energy particle irradiation. Particle irradiation of SiC leads to the formation of electrically active defects that can have an impact of the functionality of a device in terms of leakage current increase and forward voltage drop increase or the decrease of minority carrier lifetime [1, 2].

In the past, several defect characterization studies, performed by deep level transient spectroscopy (DLTS), have been carried out in particle irradiated n-type 4H-SiC. Hemmingsson et al. [3] have reported on the formation of six electrically active levels, in 2.5 MeV electron irradiated 4H-SiC. Such levels are known as EH1, EH2 (otherwise known as  $Z_{1/2}$ ), EH3, EH4, EH5, EH6/7 and reported in the 0.4-1.6 eV range, below the conduction band edge ( $E_C$ ) [3, 4, 5]. The same levels have also been detected in both 9 MeV and 15 MeV electron irradiated SiC [4, 5] and also in proton irradiated material [6, 7]. Since electrically active defects impact electronic device operation [1, 2], it is useful to understand the microscopic structure of these defects in order to find ways

to avoid them.

It is now well established that the  $Z_{1/2}$  ( $E_C$ -0.65 eV) and the EH6/7 ( $E_C$ -1.6 eV) levels are two charge states of the carbon vacancy ( $V_C$ ) [8]. The EH4 ( $E_C$ -1.03 eV) level has been associated to a cluster defect whereas the EH5 was associated to a carbon interstitial ( $C_i$ ) related defect [9]. Regarding the EH1 ( $E_C$ -0.45 eV) and EH3 ( $E_C$ -0.71 eV) levels, these are typically found in either irradiated or implanted n-type 4H-SiC and anneal out at temperatures below  $\sim$ 773 K (500°C) [10]. In 2001, Åberg et al. [11] reported the presence of the S1 level, at  $E_C$ -0.41 eV, in high temperature implanted material. Later, David et al. [6] found the S1 and also the S2 level (at around 0.7 eV below  $E_C$ ) in implanted/irradiated and annealed 4H-SiC. Both S1 and S2 anneal out at temperatures below  $\sim$ 773 K (500°C) and they are believed to be two charge states of the same defect, called S-center [6] and associated to the silicon vacancy ( $V_{Si}$ ) [12].

The presence of EH1 (EH3) and S1 (S2) has been reported in 4H-SiC epilayers after irradiation with low energy [1, 4] or high energy electrons [5, 13, 14] and also after proton [6, 15, 16] or neutron irradiation [17, 18]. Yet, since EH1 (EH3) and S1 (S2) levels share a very similar energy position in the band gap and similar annealing behavior [4, 6], the EH1 (EH3) and S1 (S2) labeling is used interchangeably in the literature [4, 7, 10, 17, 19, 20, 21, 22]. The fact that energy levels have been indistinctly identified as either EH1 (EH3) or S1 (S2), irrespective of particle energy and type, has caused inconsistency in terms of microscopic identification of EH1 and EH3, e.g., their nature was associated either to carbon [4, 13] or to silicon [17, 23] displacement.

Resolving this ambiguity is important because, recently, defects generated by particle irradiation in 4H-SiC were found to be single photon emitters [24]. This has attracted the interest of the scientific community for the development of 4H-SiC devices for quantum computing, sensing and biomedical imaging [25, 26]. To this end, the proper identification of those defects that behave as single photon sources is paramount. However, since DLTS does not allow to separate similar emission rates (closely spaced electrically active levels in the band gap), the analysis of the annealing kinetics can help to distinguish between of EH1 (EH3) and S1 (S2) and give more insight on their nature. While the annealing kinetics of S1 and S2 has been already studied in detail [6], the one of EH1 and EH3 was not. For this reason, in the present study, we carried out a detailed investigation of the annealing kinetics of EH1 and EH3 levels in electron irradiated 4H-SiC. We provide unambiguous proof that EH1 (EH3) is a different level from S1 (S2), each originating from different defect species.

## 2. Experimental details

We employed 15  $\mu$ m thick n-type nitrogen doped 4H-SiC homoepitaxial epilayers with a net-donor ( $N_d$ ) concentration of  $3\text{-}5 \times 10^{15}$  cm $^{-3}$ . As-grown samples were oxidized for 90 min at 1290°C, in order to reduce the concentration of  $Z_{1/2}$  (and EH6/7) to below the detection limit [27]. These samples were then irradiated with 116 keV electrons with a dose of  $5 \times 10^{16}$  cm $^{-2}$ . This electron energy was chosen as it is the minimum energy

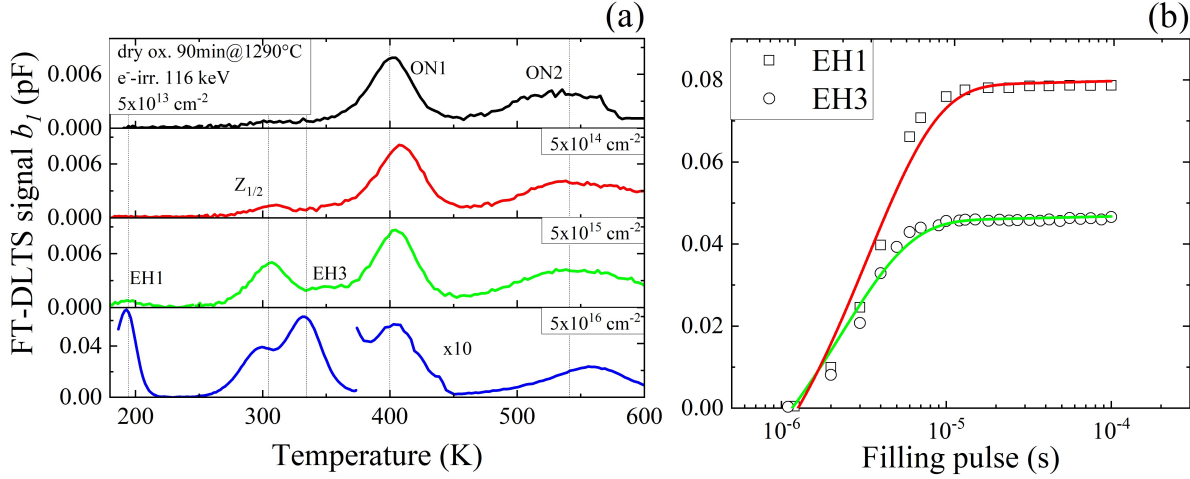


**Figure 1.** (a) FT-DLTS spectra of the oxidized and irradiated n-type 4H-SiC samples, using different doses in the  $5 \times 10^{13}$ - $5 \times 10^{16}$  cm $^{-2}$  range. The higher the dose the higher the FT-DLTS signal of EH1, Z<sub>1/2</sub> and EH3. Since the samples were oxidized, prior to irradiation, the ON1 and ON2 are also detected. Vertical dashed lines are a guide for the eye. (b) Filling pulse dependence of the FT-DLTS signal of EH1 and EH3. Red (green) solid line represent the theoretical dependence of the EH1 (EH3) signal amplitude versus filling pulse, as described by the Pons' model.

for achieving C atom displacement [4]. Another set of as-grown samples was irradiated with 116 keV electrons at room temperature with four different doses:  $5 \times 10^{13}$  cm $^{-2}$ ,  $5 \times 10^{14}$  cm $^{-2}$ ,  $5 \times 10^{15}$  cm $^{-2}$  or  $5 \times 10^{16}$  cm $^{-2}$ .

After irradiation, all samples were cleaned in HF and rinsed in de-ionized water. Schottky contacts were formed on the epilayer surface by Ni e-beam deposition while Ag paste was used on the backside as ohmic contact.

The oxidized and electron irradiated samples were subject to heat treatments in vacuum. One set of samples underwent an isochronal annealing series (time step of 15 min) in the 373-773 K (100-500°C) temperature range. Another set of samples underwent an isothermal annealing series in the 620-700 K (350-430°C) temperature range, for times ranging between 5 and 120 min.

Samples were characterized by Fourier-transform (FT-) DLTS [28] in the 100-550 K range, with a reverse bias ( $V_r$ ) of -2 V a pulse voltage ( $V_p$ ) of 2 V of the duration of 1 ms. The FT-DLTS signal consisted of the coefficient of the first sine term in the Fourier series ( $b_1$ ) with a period width ( $T_W$ ) of 0.2 s.

### 3. Results and Discussion

Fig.1 shows the results of the FT-DLTS and filling pulse dependence for the oxidized and subsequently electron irradiated samples. The FT-DLTS spectra of the oxidized 4H-SiC epilayers irradiated at different doses can be found in fig.1(a). As it can be seen, for an electron dose of  $5 \times 10^{13}$  cm $^{-2}$  the EH1 and EH3 are not found. At the same time, hints

**Table 1.** Labeling, energy position in the band gap (eV), apparent capture cross section ( $\text{cm}^2$ ) of the traps found in oxidized and irradiated ( $5 \times 10^{16} \text{ cm}^{-2}$ ) n-type 4H-SiC epilayers.

Label	$E_C - E_T$ (eV)	Capture cross section ( $\text{cm}^2$ )	Comment
EH1	$0.45 \pm 0.06$	$(6 \pm 0.02) \times 10^{-15}$	found for electron doses $\geq 5 \times 10^{15} \text{ cm}^{-2}$
$Z_{1/2}$	$0.65 \pm 0.03$	$(6 \pm 0.06) \times 10^{-16}$	$V_C$
EH3	$0.72 \pm 0.05$	$(3 \pm 0.08) \times 10^{-16}$	found for electron doses $\geq 5 \times 10^{15} \text{ cm}^{-2}$
ON1	$0.8 \pm 0.06$	$(1 \pm 0.06) \times 10^{-16}$	found after oxidation, no electron dose dependence
ON2	$1.0 \pm 0.01$	$(1.4 \pm 0.03) \times 10^{-15}$	idem

of the  $Z_{1/2}$  level are detected, whereas the ON1 ( $E_C$ -0.8 eV) and ON2 ( $E_C$ -1.0 eV) levels are clearly seen. The ON1 and ON2 are known to arise after the oxidation treatment as a result of  $C_i$  injection in the epilayer [29], so this spectrum basically coincides with that of the as-oxidized sample prior to irradiation. At a higher electron dose ( $5 \times 10^{14} \text{ cm}^{-2}$ ), the  $Z_{1/2}$  is found, together with the ON1 and ON2. The EH1 and EH3 arise only for an irradiation dose of  $5 \times 10^{15} \text{ cm}^{-2}$ . For the highest electron dose employed in this study ( $5 \times 10^{16} \text{ cm}^{-2}$ ), the EH1, EH3,  $Z_{1/2}$ , ON1 and ON2 levels are clearly distinguishable. From the Arrhenius dependence of the emission rates, we extracted the energy position in the band gap and the apparent capture cross section of EH1 and EH3. These are  $E_C$ -0.45 eV and  $6 \times 10^{-15} \text{ cm}^2$  for EH1 and  $E_C$ -0.72 eV and  $3 \times 10^{-16} \text{ cm}^2$  for EH3. The capture cross section for both levels was also measured by observing the FT-DLTS peak amplitude as a function of the filling pulse duration (fig.1(b)), in the samples irradiated with an electron dose of  $5 \times 10^{16} \text{ cm}^{-2}$ . The experimental data were then fitted by employing the Pons' model [30], which accounts for the capture kinetics at the Debye tail of the space charge region. By doing this, we obtained a value of  $\sim 10^{-17} \text{ cm}^2$  for EH1 and  $3 \times 10^{-17} \text{ cm}^2$  for EH3.

The electron dose dependence of the concentration, for all the detected levels, is displayed in fig.2. Since the  $Z_{1/2}$  is related to  $V_C$  (a primary defect) [8], the concentration of this level is expected to have a linear dose dependence [31]. As evident from the figure,  $[Z_{1/2}]$  is proportional to the 0.65 power of the electron dose (red solid line), in good agreement with the literature [32]. Having only two points in the plot, not much can be said on [EH1] and [EH3]. Yet, if they also followed a linear trend like  $Z_{1/2}$ , it could be thought that they might either related to a primary defect or to a low-order complex [31]. We also note that electron irradiation and dose variation do not affect both the presence and concentration of ON1 and ON2.

A summary of the detected traps are summarized in Table 1.

In fig.3, we show the results of the isochronal annealing series. The FT-DLTS spectra (fig.3(a)) before and after 116 keV electron irradiation, reveal the presence of five electrically active levels. In the as-grown material (dashed line in fig.3(a)), the  $Z_{1/2}$  level is found with a concentration of  $\sim 10^{12} \text{ cm}^{-3}$ . Although not entirely resolved, due to the temperature limitation of our experimental setup, hints of the EH6/7 level can

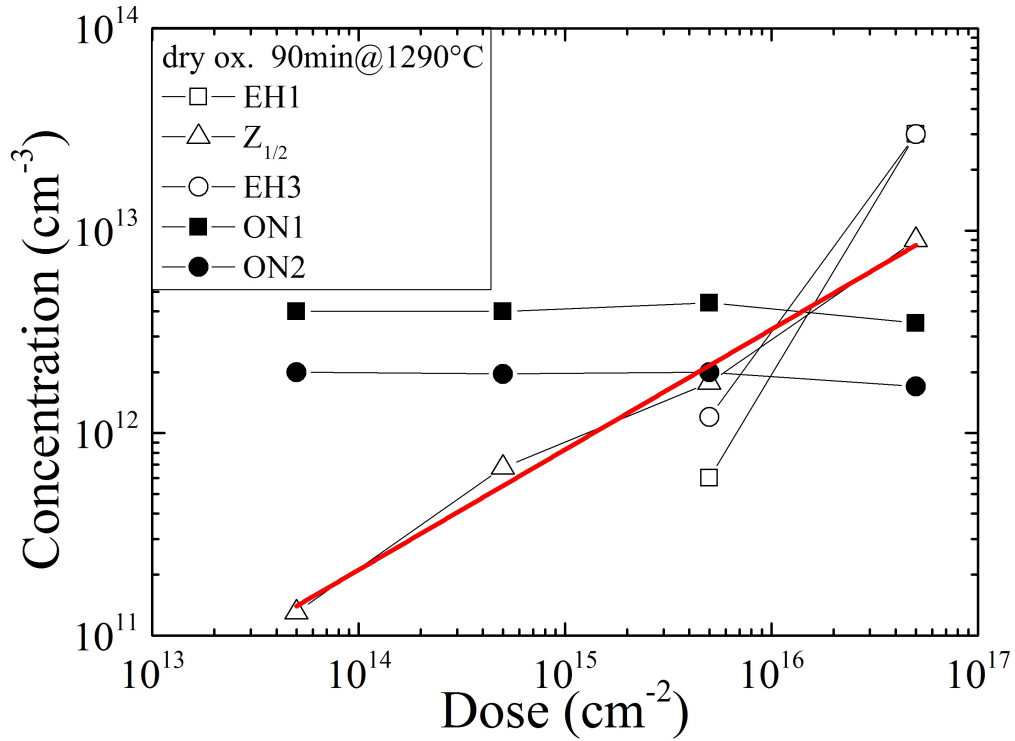


**Figure 2.** Electron dose dependence of the concentrations of EH1, Z<sub>1/2</sub>, EH3, ON1 and ON2 electrically active levels. The red solid line is the least square fitting for the [Z<sub>1/2</sub>]. No change of the concentrations of ON1 and ON2 is observed, before and after irradiation.

also be seen. After electron irradiation with a dose of  $5 \times 10^{16} \text{ cm}^{-2}$ , the concentration of Z<sub>1/2</sub> increases by one order of magnitude and the EH1 and EH3 are also detected. The EH1 and EH3 levels are also present after heat treatments up to  $\sim 473 \text{ K}$  ( $200^\circ\text{C}$ ). A strong decrease of [EH1] and [EH3] is observed after annealing at  $\sim 673 \text{ K}$  ( $400^\circ\text{C}$ ). In addition, after this annealing step, the EH5 FT-DLTS signal can also be detected at  $\sim 500 \text{ K}$ . Both EH1 and EH3 are annealed out after  $\sim 773 \text{ K}$  ( $500^\circ\text{C}$ ), while Z<sub>1/2</sub> and EH5 can still be found. The behavior of [Z<sub>1/2</sub>], [EH1] and [EH3] versus the annealing temperature is shown in fig.3(b). [Z<sub>1/2</sub>] is constant throughout the entire annealing series, in agreement with the literature [5]. On the contrary, both EH1 and EH3 anneal out at the same temperature. Their isochronal annealing behavior can be modeled by a first order annealing kinetics described by:

$$[N] = [N_0]e^{-ct} \quad (1)$$

with c, t, [N], [N<sub>0</sub>], the rate constant, the annealing time, the concentration of the defect and the concentration of the defect at t=0, respectively. The rate constant is given by:

$$c = c_0 e^{-E_a/kT} \quad (2)$$

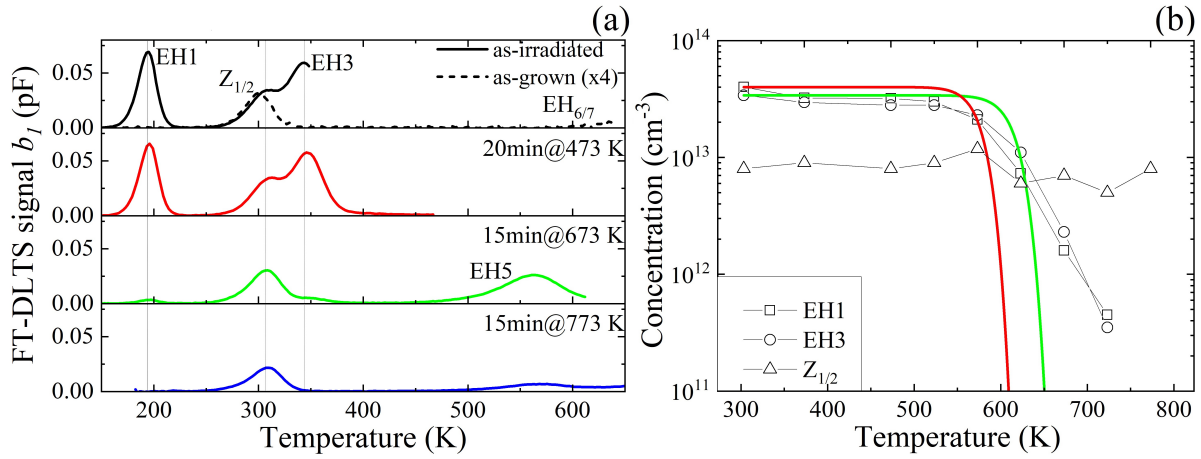


**Figure 3.** Results of (a) FT-DLTS spectra of the 116 keV electron irradiated sample ( $5 \times 10^{16} \text{ cm}^{-2}$ ), detected after different heat treatments. Black dashed line is the FT-DLTS spectrum of the as-grown material. (b) Isochronal annealing behavior of the concentrations of EH1, Z<sub>1/2</sub> and EH3, obtained from the same irradiated samples, in the 373–773 K (100–500°C) temperature range. The red (green) solid line represent the first order annealing kinetics of EH1 (EH3).

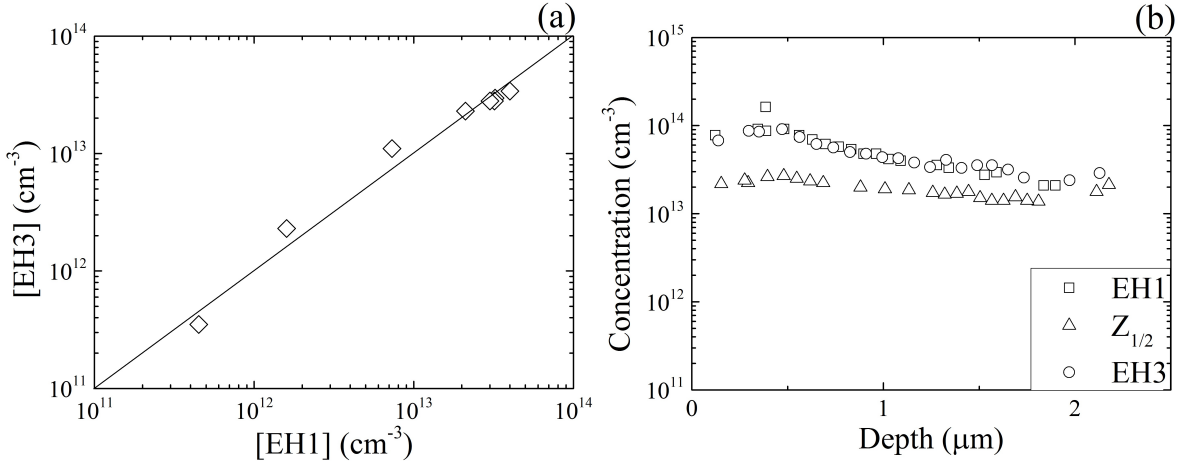
where  $c_0$ ,  $E_a$ ,  $k$  and  $T$  are the frequency factor, the activation energy, the Boltzmann constant and the annealing temperature, respectively. By modeling the annealing behavior with a  $c_0$  value of  $10^{13} \text{ s}^{-1}$  (of the order of the atomic jump frequency),  $E_a$  becomes  $1.83 \pm 0.02 \text{ eV}$  for EH1 (red solid line in fig.3(b)) and  $1.96 \pm 0.02 \text{ eV}$  for EH3 (green solid line in fig.3(b)). As the figure shows, the annealing behavior of both levels is not well reproduced. Yet, as evident from fig.3(a) and (b), the isochronal annealing behavior of both EH1 and EH3 is similar. This might suggest that, like the S1 and S2 levels, also the EH1 and EH3 might be two different charge states of the same defect.

By plotting the [EH1] versus [EH3] (fig.4(a)), we found a clear one-to-one correlation indicating that EH1 and EH3 are indeed two different charge states of the same defect. This is further confirmed by the plot of the depth profiles of EH1, EH3 and Z<sub>1/2</sub>. As fig.4(b) shows, both EH1 and EH3 profiles are indistinguishable, in the investigated depth range. The depth profile of Z<sub>1/2</sub> is also shown for comparison and has a uniform distribution.

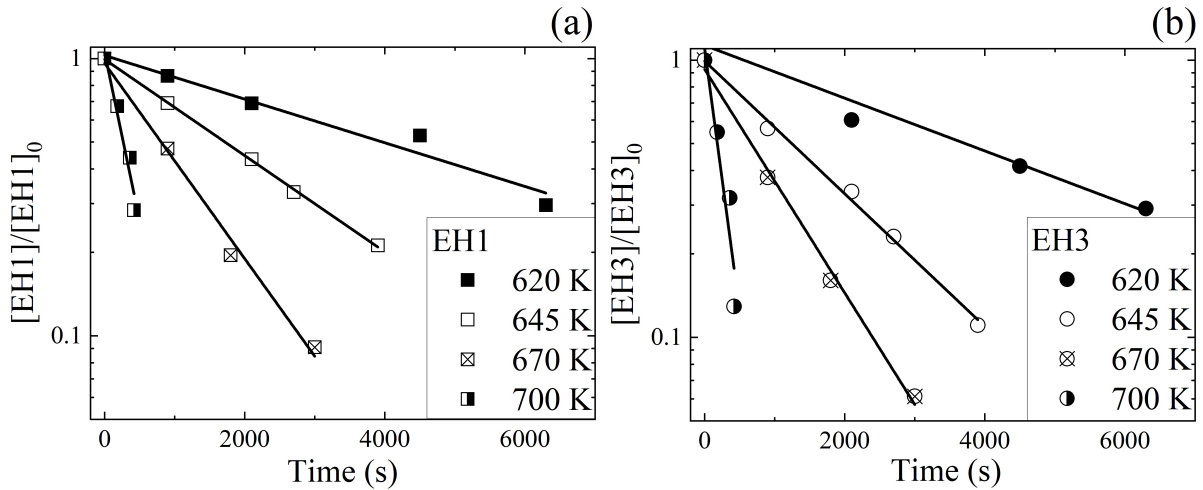
Next, we show the results of the isothermal annealing series of both EH1 and EH3. Unlike isochronal annealing studies, no a-priori assumptions on both annealing kinetics and  $c_0$  are made. In this way, it is possible to give a more detailed picture of the annealing kinetics of EH1 and EH3.

Fig.5 shows that both EH1 (fig.5(a)) and EH3 (fig.5(b)) display an exponential decrease in the 620–700 K ( $\sim 350\text{--}430^\circ\text{C}$ ) temperature range. The rate constant  $c$  exhibits an Arrhenius dependence, as described in Eq.2 and shown in fig.6, for both levels. The  $E_a$  is  $1.13 \pm 0.10 \text{ eV}$  for EH1 and  $1.17 \pm 0.15 \text{ eV}$  for EH3, further supporting the idea that these levels belong to the same defect that we label as EH-center.

In order to understand the nature of the EH-center, we first point out that the EH1 and



**Figure 4.** (a) Concentration of EH1 versus EH3, obtained from the FT-DLTS spectra of fig.3, showing a close one-to-one correlation for the two levels. (b) Depth profiles of the EH1, EH3 and  $Z_{1/2}$  levels obtained by isothermal measurements performed by varying  $V_r$  up to -30 V and by keeping a constant pulse voltage height of 2 V.



**Figure 5.** Loss of (a) EH1 and (b) EH3 versus annealing time, for the electron irradiated ( $5 \times 10^{16} \text{ cm}^{-2}$ ) samples, in the 620-700 K temperature range. The solid lines represent the least-squares fit of the experimental data.

EH3 levels arise in low-energy electron irradiated 4H-SiC (for doses  $\geq 5 \times 10^{15} \text{ cm}^{-2}$ ). The use of low energy electron irradiation (<220 keV) suggests that the detected defects are C-related because the threshold for Si-atom displacement is higher. Secondly, our isochronal annealing study has confirmed the rather low thermal stability of the EH-center which is consistent with the identification of  $C_i$ -related defects [10]. Thirdly, density functional theory studies have shown that  $C_i$  defect gives rise to two negative charged levels in the upper part of the band gap, at  $\sim E_C - 0.2 \text{ eV}$  and  $E_C - \sim 0.7 \text{ eV}$  [33]. This is also true for the carbon split interstitial  $((C_{sp})_2)$ , whose doubly and singly negative charged states were calculated to be at  $\sim E_C - 0.4 \text{ eV}$  and  $\sim E_C - 0.6 \text{ eV}$ ,

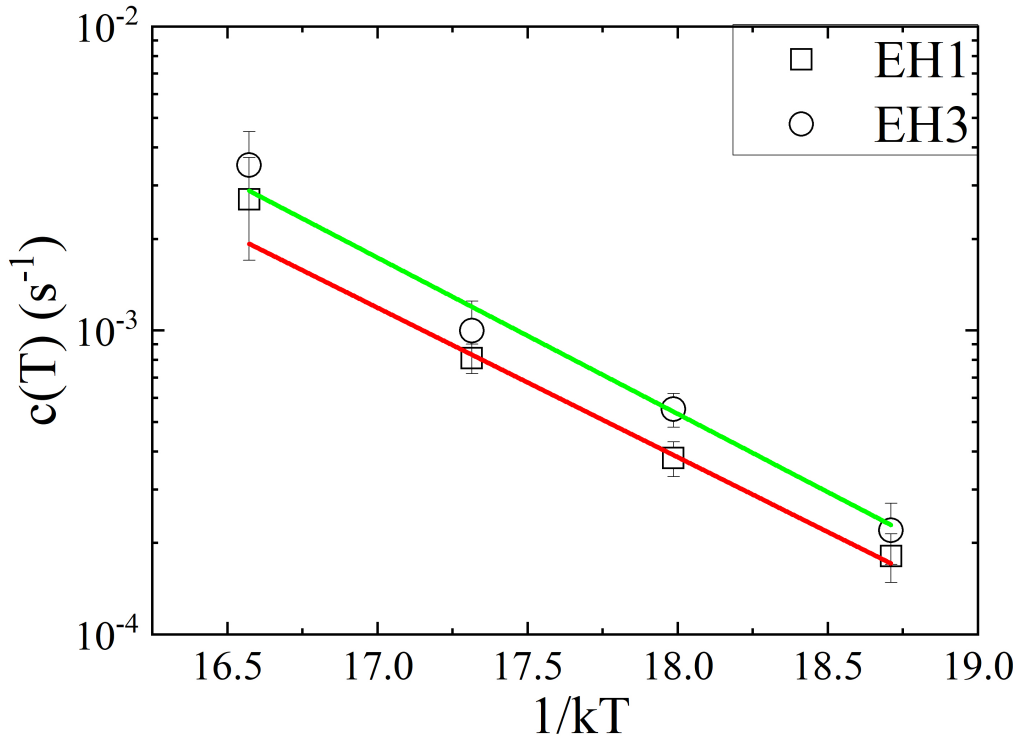


**Figure 6.** Arrhenius plot of the rate constant ( $c(T)$ ) for the annealing of EH1 and EH3. The red (green) solid line is the least-squares fit of the EH1 (EH3) experimental data.

respectively [34]. Higher order interstitial clusters can be discarded as electrically active levels of these defects were reported to be in the lower part of the band gap, closer to the valence band [35].

To further confirm the presence of C in the microscopic structure of the EH-center, we note that the value of  $c_0$ , obtained from the isothermal annealing investigation, is  $(5 \pm 0.7) \times 10^5 s^{-1}$ . This value is lower than  $kT/h$  ( $h$  is the Planck constant) suggesting that the annealing of EH-center occurs via a diffusion-limited mechanism [6, 34, 36, 37] and not via a dissociation process. A diffusion-limited mechanism can be described in two ways. We can consider a specie migrating to sinks (out-diffusing to the surface or migrating into grain boundaries) or it can be described as a specie recombining with other defects (annihilating or forming stable complexes).

By assuming a migrating specie A trapped by a center B:

$$\frac{\partial A}{\partial t} = -4\pi R(D_A + D_B)[A][B] + D_A \frac{\partial^2 A}{\partial x^2} \quad (3)$$

with  $R (5 \times 10^{-8} \text{ cm})$ ,  $D_A$  and  $D_B$  are the capture radius and the diffusivity of A and B, respectively. By considering specie A to be more mobile than B ( $D_A \gg D_B$ ) and  $[B]$  at

least one order of magnitude larger than [A] [6], then eq.3 becomes

$$\frac{\partial A}{\partial t} = -c(T)[A] \quad (4)$$

provided that  $c_0=4\pi RD_A[B]$  [37]. If we assume  $[B]=8 \times 10^{14} \text{ cm}^{-3}$  (at least one order of magnitude higher than EH-center concentration) then the diffusivity of the EH-center ( $D_A^0$ ) becomes  $9 \times 10^{-4} \text{ cm}^2/\text{s}$ . This, for a temperature of  $\sim 1320 \text{ K}$  ( $1050^\circ\text{C}$ ) corresponds to a diffusivity of  $2 \times 10^{-8} \text{ cm}^2/\text{s}$  which is similar to the diffusivity value, at the same temperature, of the  $C_i$  [37]. We point out that Kawahara et al. [29] have also reported a  $C_i$  diffusivity value of  $9.7 \times 10^{-9} \text{ cm}^2\text{s}^{-1}$ , in the  $1300\text{-}1500 \text{ K}$  range. This corresponds to energy barrier for migration of  $0.6 \text{ eV}$ , which is in agreement with the ab-initio predictions by Bockstedte et al.[34].

At last, we comment on the matter of the interchangeable EH1 (EH3) and S1 (S2) labeling, found in the literature. Despite what is commonly believed, the EH1 (EH3) level is different from the S1 (S2) for two reasons. First, the  $E_a$  for the annealing of EH1 and EH3 (EH-center) is  $\sim 1.1 \text{ eV}$ , which is  $0.7 \text{ eV}$  lower than that of S1 and S2 (S-center) [6]. Secondly, while density functional theory studies associated the nature of the S-center to  $V_{Si}$  [12], our results point to the identification of the EH-center as a C-related defect.

#### 4. Conclusions

Low-energy electron irradiation, for doses  $\geq 5 \times 10^{15} \text{ cm}^{-2}$ , gives rise to two levels in the band gap, known as EH1 and EH3. The study of the isochronal and isothermal annealing behavior showed that EH1 and EH3 are two different charge states of the same defect, called the EH-center. The EH-center anneals out with an activation energy of  $\sim 1.1 \text{ eV}$  and the analysis based on the diffusion-limited theory suggests that this defect is  $C_i$ -related. Our results indicate that the EH-center is not identifiable as the S-center which was associated to a  $V_{Si}$ -related defect.

#### 5. References

- [1] Danno K, Nakamura D, Kimoto T 2007 *Appl. Phys. Lett.* 90 202109
- [2] Kein PB 2008 *J. Appl. Phys.* 103 033702
- [3] Hemmingsson C, Son N T, Kordina O, Bergman J P, Janzén E, Lindström J L, Savage S, Nordell N 1997 *J. Appl. Phys.* 81 6155
- [4] Storasta L, Bergman J P, Janzén E, Henry A, Lu J 2004 *J. Appl. Phys.* 96 4909
- [5] Alfieri G, Monakhov E V, Svensson B G, Linnarsson M 2005 *J. Appl. Phys.* 98 043518
- [6] David M L, Alfieri G, Monakhov E V, Hallén A, Blanchard C, Svensson B G, Barbot J F, J. 2004 *Appl. Phys.* 95 4728
- [7] Martin D M, Kortegaard Nielsen H, Lévéque P, Hallén A, Alfieri G, Svensson B G 2004 *Appl. Phys. Lett.* 84 1704
- [8] Son N T, Trinh X T, Lovlie L S, Svensson B G, Kawahara K, Suda J, Kimoto T, Umeda T, Isoya J, Makino T, Ohshima T, Janzén E 2012 *Phys. Rev. Lett.* 109 187603
- [9] Sasaki S, Kawahara K, Feng G, Alfieri G, Kimoto T 2011 *J. Appl. Phys.* 109 013705

- [10] Beyer F C, Hemmingsson C, Pedersen H, Henry A, Janzén E, Isoya J, Morishita N, Ohshima T 2011 *J. Appl. Phys.* 109 103703
- [11] Åberg D, Storasta L, Hallén A, Svensson B G 2001 *Mater. Sci. Forum* 353-356 443
- [12] Gali A 2011 *Mater. Sci. Forum* 679-680 225
- [13] Castaldini A, Cavallini A, Rigutti L, Pizzini S, Le Donne A, Binetti S 2006 *J. Appl. Phys.* 99, 033701
- [14] Hazdra P, Vobecky J 2019 *phys. status solidi (a)* 216, 190312
- [15] Pastuovic Z, Siegele R, Capan I, Brodar T, Sato S, Ohshima T 2017 *J. Phys.: Condens. Matter* 29, 475701
- [16] Lovlie LS, Vines L, Svensson BG 2012 *J. Appl. Phys.* 111, 103719
- [17] Capan I, Brodar T, Yamazaki Y, OkiY, Ohshima T, Chiba Y, Hijikata Y, Snoj L, Radulovic V, 2020 *Nucl. Inst. Meth. Phys. Res. B* 478, 224
- [18] Cavallini A, Castaldini A, Nava F, Errani P, Cindro V 2006 *Mater. res. Soc. Symp. Proc.* 911, 0911-B06-01
- [19] Beyer F C, Hemmingsson C, Pedersen H, Henry A, Isoya J, Morishita N, Ohshima T, Janzén E 2010 *Mater. Sci. Forum* 645-648 435
- [20] Brodar T, Capan I, Radulovic V, Snoj L, Pastuović Z, Coutinho, J, Ohshima T 2018 *Nucl. Inst. Meth. Phys. Res. B* 437 27
- [21] Mitchel W C, Mitchell W D, Smith H E, Landis G, Smith S R, Glaser E R 2007 *J. Appl. Phys.* 101 053716
- [22] Beyer F C, Hemmingsson C, Pedersen H, Henry A, Isoya J, Morishita N, Ohshima T, Janzén E 2010 *Phys. Scr.*, 2010 014006
- [23] Zhuo X, Pandey G, Ghandi R, Losee P, Bolotnikov A, Chow TP 2019, *Mater. Sci. Forum* 963, 516
- [24] Bathen ME, Galeekas A, Müting J, Ayedh HM, Grossner U, Coutinho J, Frodason YK, Vines L 2019 *npj Quantum Information* 5 111
- [25] Fuchs F, Stender B, Trupke M, Simin D, Pflaum J, Dyakonov V, Astakhov GV 2015 *Nature Comm.* 6, 7578
- [26] Morioka N, Babin C, Nagy R, Gediz I, Hesselmeier E, Liu D, Joliffe M, Niethammer M, Dasari D, Vorobyov V, Kolesov R, Stöhr R, Ul-Hassan J, Son NT, Ohshima T, Udvarhelyi P, Thiering G, Gali A, Wrachtrup J, Kaiser F 2020 *Nature Comm.* 11, 2516
- [27] Hiyoshi T, Kimoto T 2009 *Appl. Phys. Express* 2 041101
- [28] Weiss S, Kassing R 1988 *Solid-State Electron.* 31 1733
- [29] Kawahara K, Suda J, Kimoto T 2012 *J. Appl. Phys.* 111 053710
- [30] D. Pons 1983 *J. Appl. Phys.* 55 3644
- [31] Vines L, Wong-Leung J, Jagadish C, Quemener V, Monakhov E V, Svensson B G 2012 *Appl. Phys. Lett.* 100 212106
- [32] Danno K, Kimoto T 2006 *J. Appl. Phys.* 100 113728
- [33] Gali A, Son NT, Janzen E 2006 *Phys. Rev. B* 73, 033204
- [34] Bockstedte M, Mattausch A, Pankratov O 2004 *Phys. Rev. B* 69, 235202
- [35] Mattausch A, 2005 PhD dissertation, University Erlangen-Nürnberg
- [36] Pellegrino P, Lévéque P, Lalita J, Hallén A 2001 *Phys. Rev. B* 64 195211
- [37] Løvlie L S, Svensson B G 2012 *Phys. Rev. B* 86 075205